

**SPE-200595-MS**

## **Digital Rock Physics in Low-Permeable Sandstone, Downsampling for Unresolved Sub-Micron Porosity Estimation**

Mohammad Ebadi, Ivan Makhotin, Denis Orlov, and Dmitri Koroteev, Skolkovo Institute of Science and Technology

Copyright 2020, Society of Petroleum Engineers

This paper was prepared for presentation at the SPE Europec featured at 82nd EAGE Conference and Exhibition originally scheduled to be held in Amsterdam, The Netherlands, 8-11 June 2020. The physical event was postponed until 14-17 June 2021. A virtual SPE Europec was held 1-3 December 2020 for SPE authors to present their papers. The official proceedings were published online on 8 June 2020.

This paper was selected for presentation by an SPE program committee following review of information contained in an abstract submitted by the author(s). Contents of the paper have not been reviewed by the Society of Petroleum Engineers and are subject to correction by the author(s). The material does not necessarily reflect any position of the Society of Petroleum Engineers, its officers, or members. Electronic reproduction, distribution, or storage of any part of this paper without the written consent of the Society of Petroleum Engineers is prohibited. Permission to reproduce in print is restricted to an abstract of not more than 300 words; illustrations may not be copied. The abstract must contain conspicuous acknowledgment of SPE copyright.

### **Abstract**

The approach to handle the unresolved pores at 3D X-ray Micro Computed Tomography ( $\mu$ CT) images of core samples is developed. It enables a sufficient widening of digital rock studies for tight rocks. The  $\mu$ CT images of a low-permeable sandstone with a resolution of 1.2  $\mu\text{m}/\text{voxel}$  have been generated. Pore Size Distribution shows the presence of a significant amount of sub-resolution pores. Downsampling has been applied to estimate the actual porosity with extrapolation.

Visual noise, artifacts, and roundoff errors are the major factors affecting the quality of  $\mu$ CT images. We apply transform and spatial domain filtering to minimize all the artifacts. Regarding the overall concept of porosity and through running a geometrical histogram analysis, the Random Walker segmentation as a robust mathematical algorithm has been applied to turn the greyscale  $\mu$ CT images into binary ones resembling pores and grains. Next, the porosity of the binary images with a resolution of 1.2  $\mu\text{m}/\text{voxel}$  has been calculated. The procedure continues with downsampling to artificially reduce the resolution and calculate the corresponding porosity.

It has been observed that the calculated porosity for the highest resolution of 1.2 micrometer is still lower than the experimental value which is due to the existence of pores which their sizes are less than 1.2 micrometer, and cannot be seen in the CT images. In order to take the effects of sub-resolution pores into account, an extrapolation relying on the downsampling technique has successfully been applied. The implemented technique is based on the fact that the porosity of the reservoir rock sample is not a function of resolution. However, plotting of the calculated porosities versus their relevant resolutions indicates that the value of porosity has an inverse relationship with the voxel size. In other words, it could be interpreted that the closest values of the calculated porosity to the laboratory reports will be the output of the image processing when the size of voxel moves towards zeros as much as possible, which is technically impossible. Instead, a trendline can be fitted into the scatter plot of porosity versus resolution and find its extrapolation value for the voxel size of zero, which provides the porosity as close as possible to the experimental value.

The main logic behind the digital core analysis is to calculate the properties only according to the digital images. Although there are some studies in which modifications have been done to consider the effects of sub-resolution pores, they are severely suffering from mathematical complexities, and they are mainly

based on the global thresholding. The proposed technique can provide an accurate value of porosity when there are no additional data about the pore structure of the sub-micron scale.

## Introduction

Based on the recent incredible advances in various fields of reservoir stimulations, well completion, and drilling technologies developments of tight and ultra-tight hydrocarbon resources have been considered as the backbone of booming economies in the world (Ahmadi et al., 2014; Ebadi and Koroteev, 2019). Accordingly, the leading oil companies of the global energy perspective put forth great efforts to have commercial and stable production from the abovementioned hydrocarbon resources in which the initial reserves are enormously more significant than the reserve of conventional resources (Bezyan et al., 2019). Despite all the eye-catching technological achievements, the development of unconventional resources might yet be a risky investment if it is not supported well with detailed and accurate reservoir studies (Wang et al., 2019). As a result and subject to the requirements of reservoir studies and relevant challenges, developing techniques, methods, and instruments for the comprehensive evaluation of unconventional hydrocarbon studies is currently an important area of research (Li et al., 2019).

Regardless of many attempts that have been made to modify the conventional methods of core analysis suitable to be applied for the evaluation of unconventional hydrocarbon resources (Lu et al., 2020), they are still time-consuming, expensive, and inaccurate (Sander et al., 2017). It is mainly due to the existence of sub-micron pores and throats that have strong effects on the storage and flow of tight and ultra-tight oil and gas resources (Chai et al., 2019; Javadpour, 2009). Not only they provide extensive exposed surface areas suitable for a considerable amount of adsorbed gas affecting the storage mechanisms (Allawe et al., 2015), but also they reject the idea of applying Darcy's law, which has initially been developed for micro-scale pores (Yu et al., 2016).

To fit the risk attitude of the decision-makers, applying modern methods of core analysis like Digital Rock Physics (DRP) has mainly been focused over the last decade (Kelly et al., 2016; Zhang et al., 2019). Besides the fact that DRP is an efficient method of cost control and risk management, it provides the research projects with the opportunities of performing multiple numerical experiments on exactly the same sample and implementing various analyses on one sample at the same time (Jia et al., 2016; Verri et al., 2017).

As a non-destructive method, the DRP workflow begins with projecting a rotating sample with the X-ray (Al-Marzouqi, 2018). The generated sinograms are fed to the algorithm of tomographic reconstruction, which is typically a multidimensional inverse problem to produce an estimate of a specific system from a finite number of projections (Chauhan et al., 2016). Then, the Computed Tomography (CT) images are processed with denoising algorithms, mainly according to spatial and transform domain filtering (Diwakar and Kumar, 2018). As a consequence of applying the segmentation algorithm, the filtered grayscale images are turned into black and white images resembling pores and grains, respectively (Zaitoun and Aqel, 2015). The finalized structure is then considered as the representation of the rock for further numerical simulations of other important petrophysical parameters (Halisch et al., 2016).

The spatial resolution of CT images shows the ability to distinguish between objects or structures that differ in density (Saxena et al., 2018). The CT images of unconventional samples with the spatial resolution of  $\mu\text{m}/\text{voxel}$  cannot indicate the sub-micron pores (Goral et al., 2020). Although increasing the resolution can show more details, the Field Of View (FOV) decreases, causing the generated images losing their representativeness (Sudakov et al., 2019). The referred trade-off should be considered as careful as possible; otherwise, the subsequent calculations will suffer from inaccuracy and lack of regarding enough details.

A couple of research have tried to take the effects of sub-resolved pores into account during the DRP calculations. By coupling the advantages of  $\mu\text{CT}$  and QEMSCAN (Quantitative Evaluation of Minerals by SCANNing electron microscopy) images, representative 3D mineralogy, and porosity maps were reconstructed by Rusipini et al. (2016). Then, the reconstructed maps were employed to obtain a Multi-Scale

Pore Network (MSPN) representing both micro- and macro-porosity regions. Eventually, a Process-Based Method (PBM) was applied to the extracted MSPN to characterize the favorite petrophysical properties (Ruspini et al., 2016). The petrophysical properties for different rock types varying from sandstone to carbonate samples have been studied (Shah et al., 2016). The samples were firstly scanned at four different resolutions, and then the generated images were fed to the two modeling techniques of Lattice Boltzmann Method (LBM) and Pore Network Modeling (PNM) for further calculation of permeability. Next, a numerical coarsening method was applied, which artificially reduces the resolution of images. The synthetically reduced-resolution images have been reintroduced to the supposed algorithm. The generated results showed the same accuracy for the favorite parameters. Therefore, it has been deduced that numerical coarsening can be considered as an essential asset in improving the computational efficiency of transport property calculations.

Technically, the numerical coarsening or generally known as downsampling is one of the main image processing methods in which the spatial resolution is going to be reduced while keeping the same i-dimensional representation (Frajka and Zeger, 2004). Regarding a signal as  $x = (x_n)$ , downsampling  $x$  by  $n$  can be commonly viewed as pre-filtering  $x$  with a linear filter  $g = (g_k)$ , generating a signal  $u = (u_n)$ , and then decimating  $u$  by  $i$ , receiving a signal  $v = (v_n)$  where  $v_n = u_{in}$  for all  $n$  (Eklund et al., 2013).

The current research has firstly shown that applying the downsampling method to analyze the petrophysical properties of a tight formation causes the generation of results unquestionably in contrast with previous studies. Then, the introduced method has innovatively been employed to extract the actual porosity of the gathered tight samples in which the porosities of their micro-scale CT images are not trustworthy because of not taking the effects of sub-micron pores into account. The methodology will discuss more details about the applied downsampling method and how it can help to estimate the actual porosity. Then, the results of implementing the introduced method of four different samples are shown. The conclusion is that downsampling on tight formation is a considerable method that can effectively be implemented to find true porosities.

## Methodology

Firstly, the supposed core sample should rotationally be projected with the X-ray. Then, the tomographic reconstruction of projection images leads to a 3D map of X-ray absorption, Figure 1. Because features and phases of different materials often have various X-ray absorption properties, the supposed constructing elements can accordingly be identified from the images. Obtained back-projected images with different angles in which brightness depends on the degree of X-ray absorption are then superimposed to reconstruct the 3D digital model (Blunt et al., 2013).

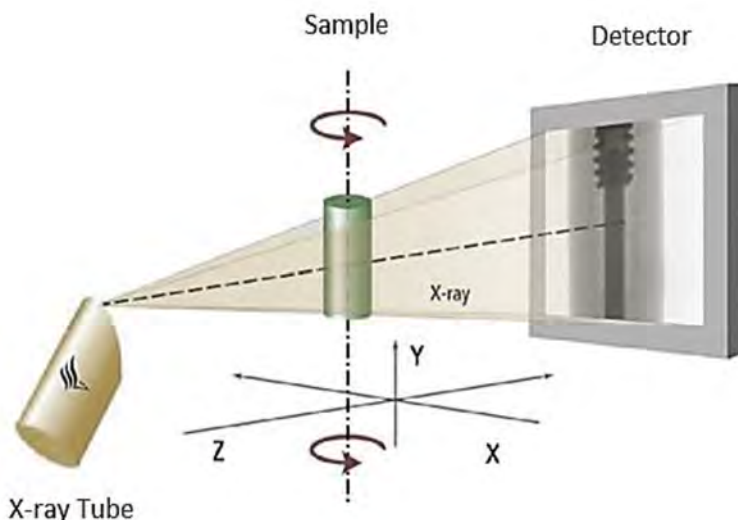


Figure 1—Experimental procedure of X-ray projection

The reconstruction of a 3D object from a series of 2D projections at different angles is the essential element of modern imaging methods. The supposed 3D object can be created as the result of stacking the sequence of tomographically reconstructed 2D images. The existence of artifacts, roundoff errors, and different types of visual or mathematical noises in the reconstructed CT images are the main reasons to build incorrect 3D digital models of the pore network structure (Alqahtani et al., 2020).

In general, it is assumed that a noisy image is a combination of the noise component and an original image. Thus, applying edge-preserving denoising approaches is highly essential to improve the quality of the CT images. However, there is a trade-off between noise reduction and the preservation of actual contents. In other words, the main challenging task is to reduce the level of noise without losing significant features such as sharp structures, corners, and edges. Avoiding the generation of new artifacts and preservation of image boundaries are the main goals of mathematical algorithms named as filters to suppress the noises from CT images (Jin et al., 2018).

Image denoising can be categorized based on two primary methods of spatial or transform domain filtering. In spatial domain filtering, the target is to reduce noises by applying the filtering process directly on the original noisy images. There is no doubt that Bilateral filters are one of the most prominent subsets of spatial domain filtering. By applying bilateral filters, the intensity values of voxels in each image are replaced by a weighted average of intensity values from surrounding voxels. As the second group, transform domain filtering methods are typically Fourier transformed, multiplied with the filter function, and then re-transformed into the spatial domain. As one of the most commonly used method, the bandpass filter removes noise and background variation. It attenuates very low and very high frequencies but retains a middle-range band of frequencies (Reshetova et al., 2019).

Besides, the main idea of DRP is based on the fact that each porous media could be considered as being the union of solid and empty parts. Accordingly, the segmentation techniques should be applied to the denoised gray-scale CT images to turn them into black and white versions resembling pores and grains, respectively. To develop a robust segmentation algorithm capable of overcoming the mentioned difficulties, taking advantage of statistical particle-based methods has drawn many researchers' attention. Accordingly, applications of Random Walker (RW) theory has innovatively provided the communities of image processing with highly efficient and practical segmentation algorithms. Receiving binary images in which even weak boundaries are respected is the eye-catching output of applying RW theory as the segmentation algorithm where occurrences of crossing the sharp intensity gradients have been avoided by consideration of imposing biases to the main body of the procedure (Grady, 2006).



Due to the thresholding nature of the binarization technique, some voxels attributable to grains can instead be classified as the pore space and vice versa. In order to improve the quality of binarised outputs and address the abovementioned commonly occurring visual artifacts, it is highly recommended to take advantage of morphological transformations, which are some shift-invariant operators strongly related to Minkowski additions (Shaik et al., 2019). In more details, Dilation and Erosion are the fundamental operators that are the basis for other similar operators as well. In the Erosion, supposed voxels locating in the center of the kernel is the minimum of the remaining elements of the kernel. On the other hand, values of the voxels in the Dilation are the maximum of other elements of the kernel. The procedure of image processing mentioned above has schematically been illustrated in Figure 2.

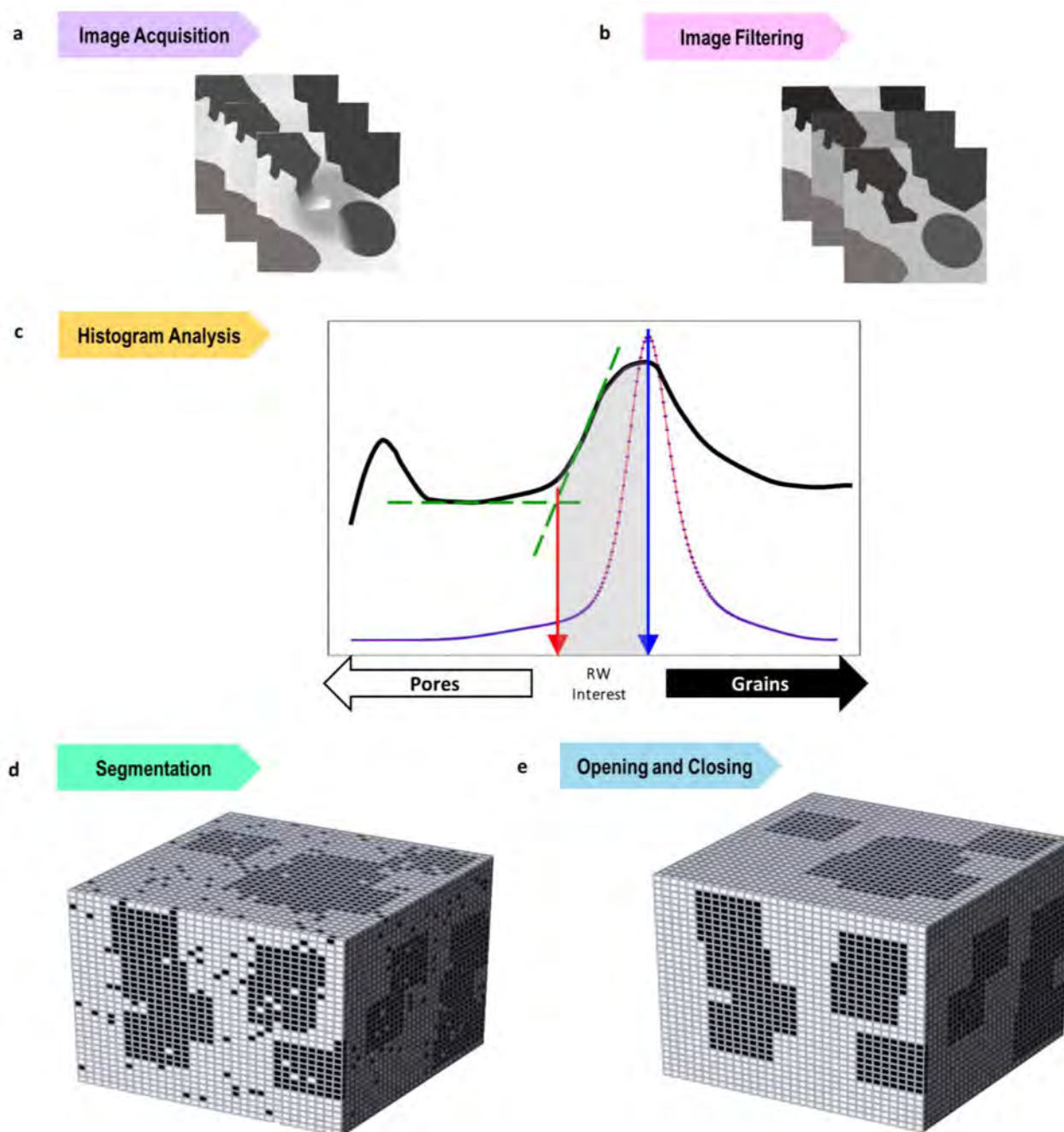


Figure 2—The workflow of digital image processing

Following the main concept of downsampling, the finalized binary cubes of different samples having the high resolution are sequentially applied with the coarsening algorithm. The description of the coarsening algorithm relies on the concept of turning  $2^3$  neighboring voxels into a single cube based on the maximum operator. The result is a downsampled cube that has the same physical length but with a two times lower resolution. After calculating the porosity of the formed cube, the algorithm proceeds to the next step where the previous downsampled cube undergoes the next step of resolution reduction, which its output has a four times lower resolution. The algorithm has graphically been illustrated in Figure 3.

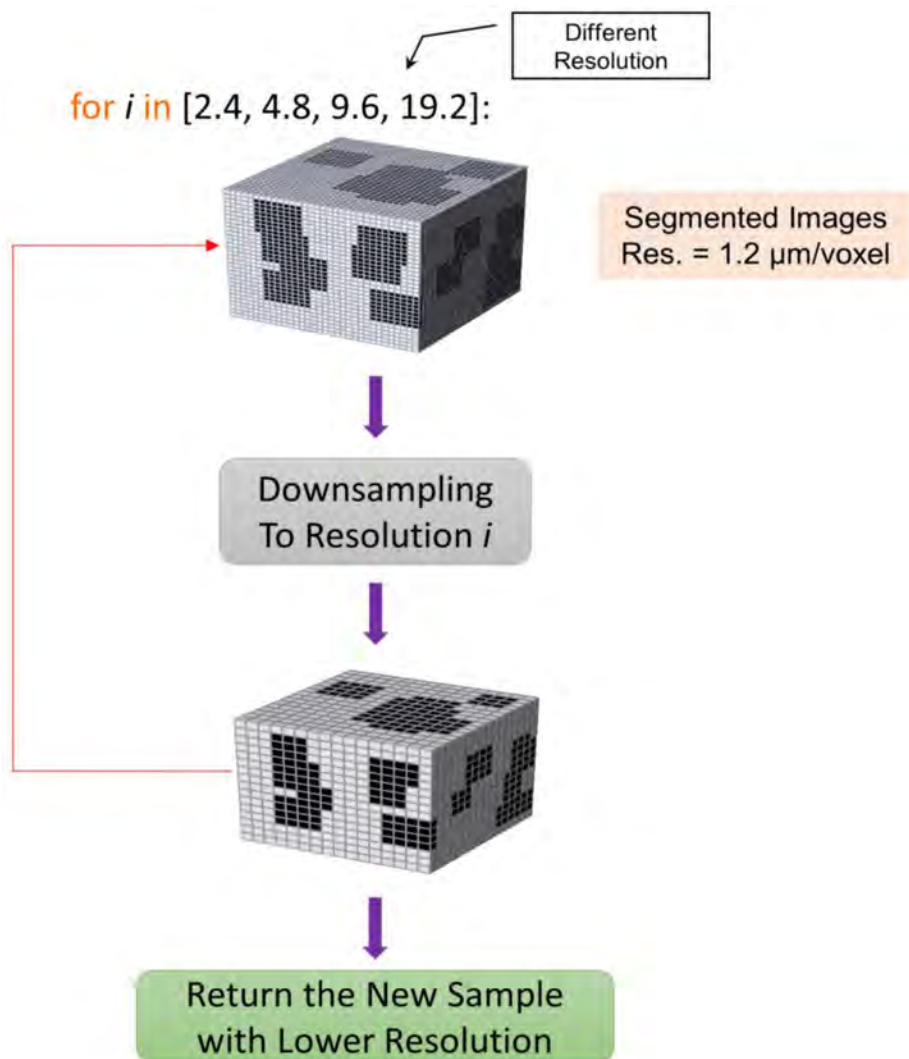


Figure 3—The sequential Downsampling

After having the finalized binary cube and the downsampled representations, the porosity of each one can be calculated through the ratio of black voxels over the total number of voxels. Then, an exponential trendline is fitted to the scatter plot of porosity versus resolution for each sample. The intersection of the trendline with the y-axis, where the resolution has its highest theoretical value of  $0 \mu\text{m}/\text{voxel}$ , shows the porosity very close to the experimental values for tight sandstones. The described procedure has schematically been shown in Figure 4.

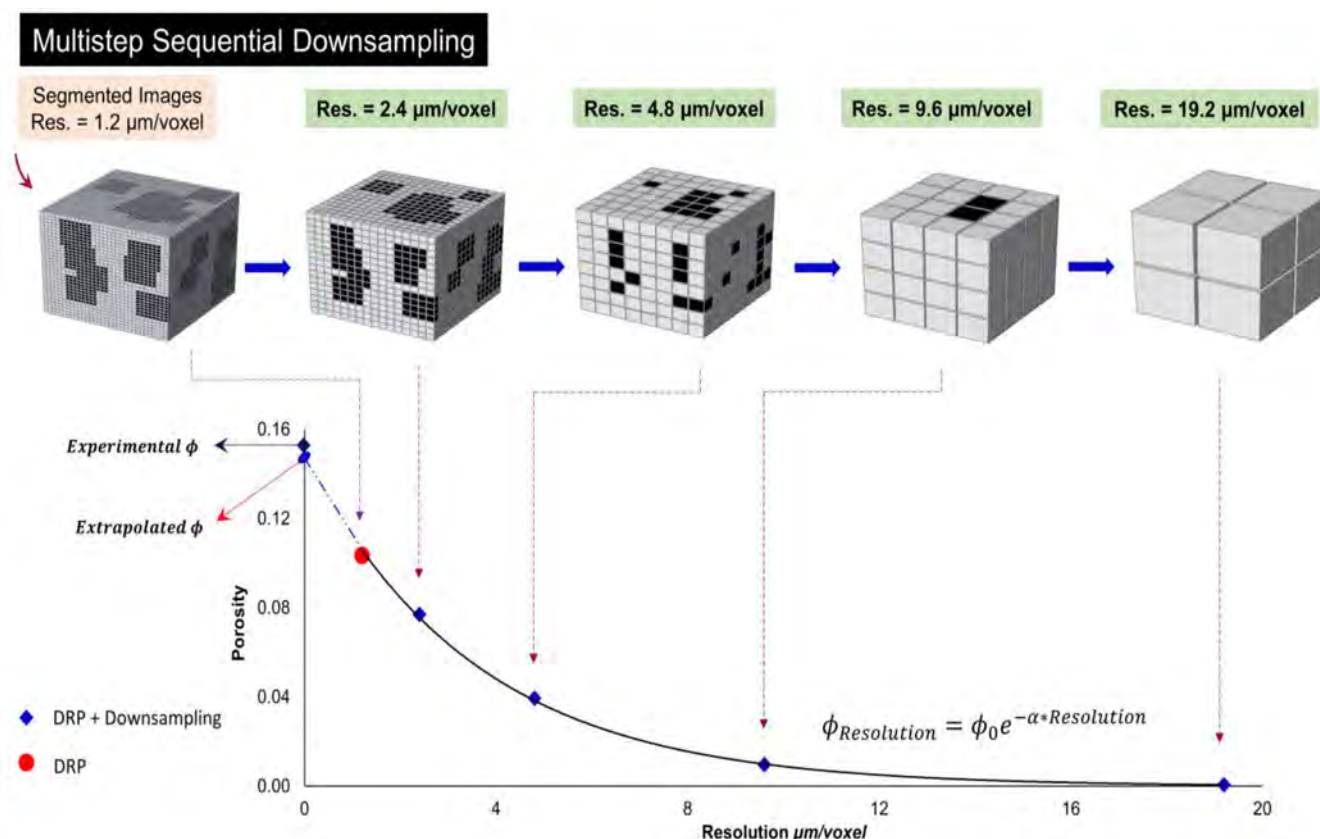
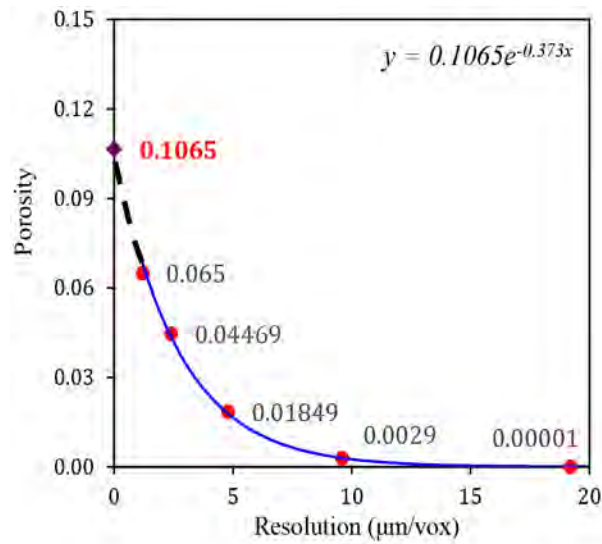


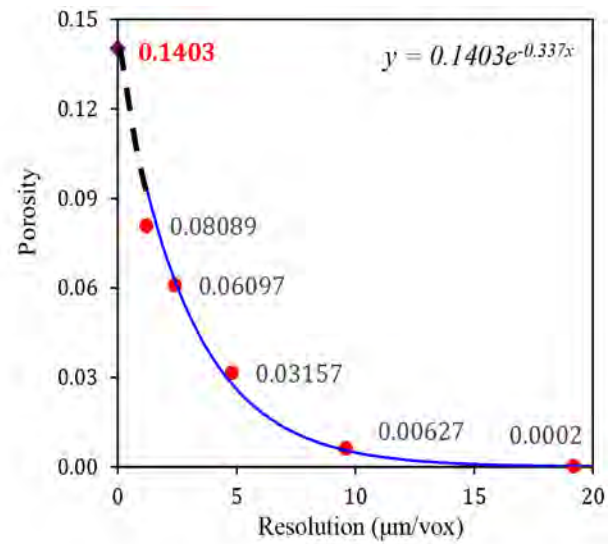
Figure 4—Implementation of image processing to take effects of sub-resolved pores into account

## Results and Discussions

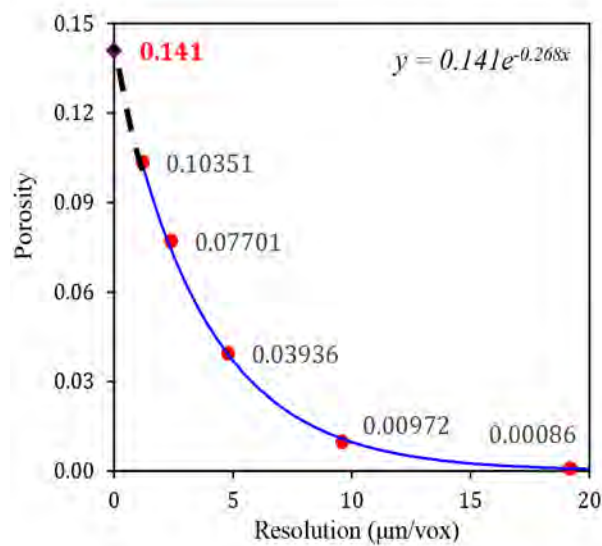
As a tight formation, four core samples have been gathered from the Achimovka formation located in Siberia, Russia (Yakimchuk et al., 2019). Running the tomography construction based on the focused X-ray projection leads to generating a series of 8-bit unsigned gray-scale images having a spatial resolution of 1.2  $\mu\text{m}/\text{voxel}$ . Then, the abovementioned workflow of image processing was applied, which its results for one of the images have been shown in Figure 5. The porosities of formed cubes based on binary images having a size of  $1400^3$  have been reported in Table 1. The results for all samples show that applying the DRP method even based on high-resolution images leads to generate results suffering from noticeable underestimation shown by the average relative error of  $-36\%$ .



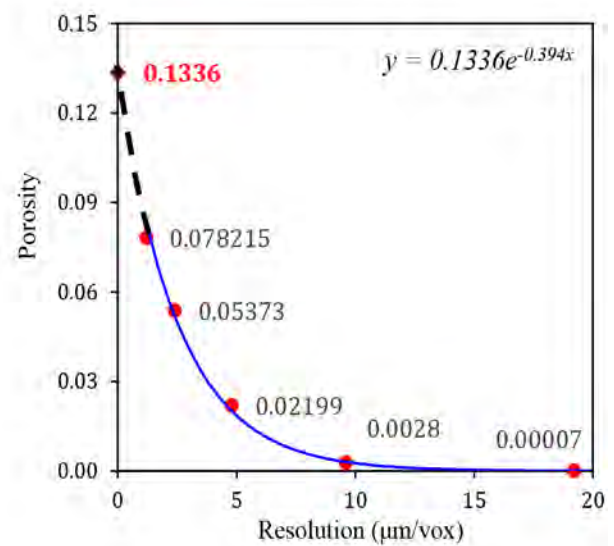
(a)



(b)



(c)



(d)

Figure 5—The intersection of the extrapolated correlation with the y-axis of porosity for different samples - (a) A15 (b) A11 (c) A13 (d) A24

Table 1—Calculated porosities of digital samples with the resolution of 1.2 μm/voxel and the corresponding relative errors based on the experimental values

Sample	Experimental $\phi$	Calculated $\phi$	Relative Error
A15	0.107	0.0650	-39.25%
A11	0.139	0.0808	-41.80%
A13	0.136	0.1035	-23.88%
A24	0.127	0.0782	-38.41%



Following the pictured algorithm in Figure 3, each cube was fed to the sequential downsampling algorithm, and then 4 more cubes having the same physical dimensions but with different lower resolutions were generated. The calculated porosities were plotted versus their corresponding resolutions, and then they were fitted with an exponential equation like what has been shown in Figure 4. According to the fact that the theoretical resolution of 0  $\mu\text{m}/\text{voxel}$  provides us with the most accurate information, the fitted correlation was extrapolated to the resolution of zero. The subsequent intersection with the porosity-axis was taken as the value to be compared with the experimental porosity. The results have been represented in Figure 5. It should be considered that in contrast with the previous studies of conventional samples, the porosities of downsampled tight cubes are a strong function of the supposed resolution. The extracted values and their corresponding relative errors have been reported in Table 2. The average relative error of 2.33% for the porosities of downsampled cubes shows that the proposed algorithm for the tight resources can generate results much more satisfying than the implementation of classic DRP. It is shown in Figure 6 where the generated relative errors of both algorithms for each sample have simultaneously been compared.

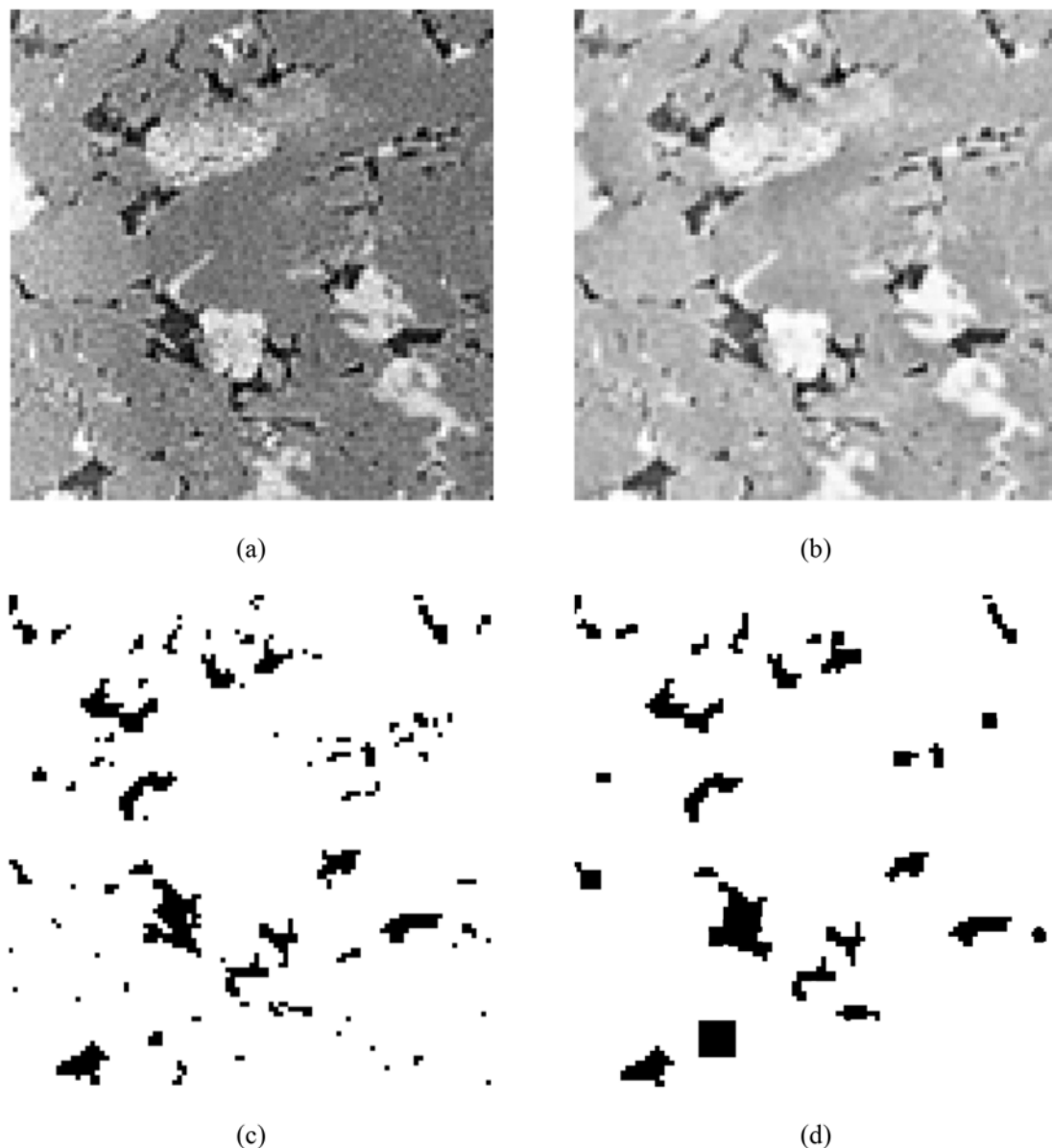


Figure 5—The intersection of the extrapolated correlation with the y-axis of porosity for different samples - (a) A15 (b) A11 (c) A13 (d) A24

Table 2—Extrapolated porosities of Downsampled cubes and the corresponding relative errors based on the experimental values

Sample	Experimental $\phi$	Extrapolated $\phi$	Relative Error
A15	0.107	0.107	-0.47%
A11	0.139	0.140	0.94%
A13	0.136	0.141	3.68%
A24	0.127	0.134	5.20%

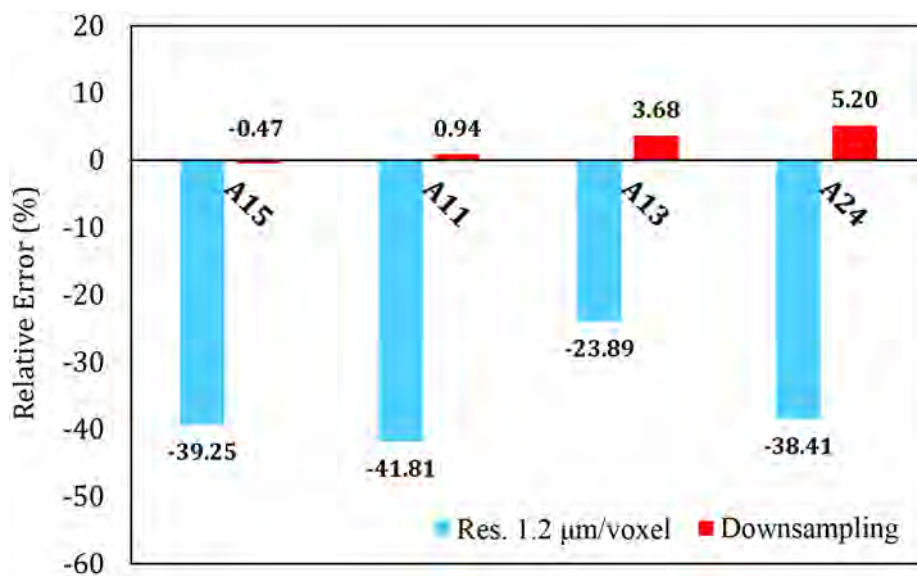


Figure 6—The comparison of classic DRP versus Downsampling method

## Conclusions

The current research has proposed a downsampling-based algorithm to estimate the porosity of tight samples in which a noticeable portion of pores has the nano-scale size and cannot be detected by the microscale DRP methods. Although the results of applying the DRP based on high-resolution images are not satisfying at all, the generated outputs of the launched technique are in a strong agreement with the experimental values. The results indicate that the represented method can effectively be employed to analyze the porosity and other favorite parameters of tight sandstones in which there is a large portion of sub-micron pores that cannot be detected in microscale CT images.

## References

- Ahmadi, M.A., Ahmadi, M.R., Hosseini, S.M., Ebadi, M., 2014. Connectionist model predicts the porosity and permeability of petroleum reservoirs by means of petro-physical logs: Application of artificial intelligence. *Journal of Petroleum Science and Engineering* **123**, 183–200. [10.1016/j.petrol.2014.08.026](https://doi.org/10.1016/j.petrol.2014.08.026)
- Al-Marzouqi, H., 2018. Digital Rock Physics: Using CT Scans to Compute Rock Properties. *IEEE Signal Processing Magazine* **35**, 121–131. [10.1109/MSP.2017.2784459](https://doi.org/10.1109/MSP.2017.2784459)
- Allawe, E.M., Stockdale, A.P., Aminiaa, K., Amen, S., 2015. Impact of Nanoscale Pore Confinement on Estimation of Gas Resources and Gas/Condensate Behavior in Shale Reservoirs, in: SPE Eastern Regional Meeting. *Society of Petroleum Engineers*. [10.2118/177285-MS](https://doi.org/10.2118/177285-MS)
- Alqahtani, N., Alzubaidi, F., Armstrong, R.T., Swietojanski, P., Mostaghimi, P., 2020. Machine learning for predicting properties of porous media from 2d X-ray images. *Journal of Petroleum Science and Engineering* **184**, 106514. [10.1016/J.PETROL.2019.106514](https://doi.org/10.1016/J.PETROL.2019.106514)
- Bezryan, Y., Ebadi, M., Gerami, S., Rafati, R., Sharifi, M., Koroteev, D., 2019. A novel approach for solving nonlinear flow equations: The next step towards an accurate assessment of shale gas resources. *Fuel* **236**, 622–635. [10.1016/j.fuel.2018.08.157](https://doi.org/10.1016/j.fuel.2018.08.157)

- Blunt, M.J., Bijeljic, B., Dong, H., Gharbi, O., Iglauer, S., Mostaghimi, P., Paluszny, A., Pentland, C., 2013. Pore-scale imaging and modelling. *Advances in Water Resources* 51, 197–216. [10.1016/J.ADVWATRES.2012.03.003](https://doi.org/10.1016/J.ADVWATRES.2012.03.003)
- Chai, D., Fan, Z., Li, X., 2019. A New Unified Gas-Transport Model for Gas Flow in Nanoscale Porous Media. *SPE Journal* 24, 698–719. [10.2118/194208-PA](https://doi.org/10.2118/194208-PA)
- Chauhan, S., Riihaak, W., Anbergen, H., Kabdenov, A., Freise, M., Wille, T., Sass, I., 2016. Phase segmentation of X-ray computer tomography rock images using machine learning techniques: an accuracy and performance study. *Solid Earth* 7, 1125–1139. [10.5194/se-7-1125-2016](https://doi.org/10.5194/se-7-1125-2016)
- Diwakar, M., Kumar, M., 2018. A review on CT image noise and its denoising. *Biomedical Signal Processing and Control* 42, 73–88. [10.1016/j.bspc.2018.01.010](https://doi.org/10.1016/j.bspc.2018.01.010)
- Ebadi, M., Koroteev, D., 2019. Towards a Reliable Determination of Saturation Pressure: A Hybrid of Mouth Brooding Fish MBF Algorithm and Flash Calculations, in: SPE/IATMI Asia Pacific Oil & Gas Conference and Exhibition. *Society of Petroleum Engineers*. [10.2118/196427-MS](https://doi.org/10.2118/196427-MS)
- Eklund, A., Dufort, P., Forsberg, D., LaConte, S.M., 2013. Medical image processing on the GPU — Past present and future. *Medical Image Analysis* 17, 1073–1094. [10.1016/J.MEDIA.2013.05.008](https://doi.org/10.1016/J.MEDIA.2013.05.008)
- Frajka, T., Zeger, K., 2004. Downsampling dependent upsampling of images. *Signal Processing: Image Communication* 19, 257–265. [10.1016/J.IMAGE.2003.10.003](https://doi.org/10.1016/J.IMAGE.2003.10.003)
- Goral, J., Andrew, M., Olson, T., Deo, M., 2020. Correlative core- to pore-scale imaging of shales. *Marine and Petroleum Geology* 111, 886–904. [10.1016/J.MARPETGEO.2019.08.009](https://doi.org/10.1016/J.MARPETGEO.2019.08.009)
- Grady, L., 2006. Random Walks for Image Segmentation. *IEEE Transactions on Pattern Analysis and Machine Intelligence* 28, 1768–1783. [10.1109/TPAMI.2006.233](https://doi.org/10.1109/TPAMI.2006.233)
- Halisch, M., Steeb, H., Henkel, S., Krawczyk, C.M., 2016. Pore-scale tomography and imaging: applications, techniques and recommended practice. *Solid Earth* 7, 1141–1143. [10.5194/se-7-1141-2016](https://doi.org/10.5194/se-7-1141-2016)
- Javadpour, F., 2009. Nanopores and Apparent Permeability of Gas Flow in Mudrocks (Shales and Siltstone). *Journal of Canadian Petroleum Technology* 48, 16–21. [10.2118/09-08-16-DA](https://doi.org/10.2118/09-08-16-DA)
- Jia, C., Zheng, M., Zhang, Y., 2016. Some key issues on the unconventional petroleum systems. *Petroleum Research* 1, 113–122. [10.1016/S2096-2495\(17\)30036-4](https://doi.org/10.1016/S2096-2495(17)30036-4)
- Jin, X., Yu, C., Wang, X., Liu, X., Li, J., Jiao, H., Su, L., 2018. Multi-Scale Digital Rock Quantitative Evaluation Technology on Complex Reservoirs, in: SPE Asia Pacific Oil and Gas Conference and Exhibition. *Society of Petroleum Engineers*. [10.2118/191878-18APOG-MS](https://doi.org/10.2118/191878-18APOG-MS)
- Kelly, S., El-Sobky, H., Torres-Verdin, C., Balhoff, M.T., 2016. Assessing the utility of FIB-SEM images for shale digital rock physics. *Advances in Water Resources* 95, 302–316. [10.1016/j.advwatres.2015.06.010](https://doi.org/10.1016/j.advwatres.2015.06.010)
- Li, S., Sang, Q., Dong, M., Luo, P., 2019. Determination of inorganic and organic permeabilities of shale. *International Journal of Coal Geology* 215, 103296. [10.1016/j.coal.2019.103296](https://doi.org/10.1016/j.coal.2019.103296)
- Lu, X., Armstrong, R.T., Mostaghimi, P., 2020. Analysis of gas diffusivity in coal using micro-computed tomography. *Fuel* 261, 116384. [10.1016/j.fuel.2019.116384](https://doi.org/10.1016/j.fuel.2019.116384)
- Reshetova, G., Cheverda, V., Lisitsa, V., Khachkova, T., 2019. Multiscale Digital Rock Modelling for Reservoir Simulation, in: SPE/IATMI Asia Pacific Oil & Gas Conference and Exhibition. *Society of Petroleum Engineers*. [10.2118/196561-MS](https://doi.org/10.2118/196561-MS)
- Ruspini, L.C., Lindkvist, G., Bakke, S., Alberts, L., Carnerup, A.M., Oren, P.E., 2016. A Multi-Scale Imaging and Modeling Workflow for Tight Rocks, in: SPE Low Perm Symposium. *Society of Petroleum Engineers*, 5–6. [10.2118/180268-MS](https://doi.org/10.2118/180268-MS)
- Sander, R., Pan, Z., Connell, L.D., 2017. Laboratory measurement of low permeability unconventional gas reservoir rocks: A review of experimental methods. *Journal of Natural Gas Science and Engineering* 37, 248–279. [10.1016/j.jngse.2016.11.041](https://doi.org/10.1016/j.jngse.2016.11.041)
- Saxena, N., Hows, A., Hofmann, R., Alpak, F., Freeman, J., Hunter, S., Appel, M., 2018. Imaging and computational considerations for image computed permeability: Operating envelope of Digital Rock Physics. *Advances in Water Resources* 116, 127–144. [10.1016/J.ADVWATRES.2018.04.001](https://doi.org/10.1016/J.ADVWATRES.2018.04.001)
- Shah, S.M.M., Gray, F., Crawshaw, J.P.P., Boek, E.S.S., 2016. Micro-computed tomography pore-scale study of flow in porous media: Effect of voxel resolution. *Advances in Water Resources* 95, 276–287. [10.1016.2015.07.012](https://doi.org/10.1016.2015.07.012)
- Shaik, A.R., Al-Ratrou, A.A., AlSumaiti, A.M., Mani, A.K., 2019. Rock Classification Based on Micro-CT Images using Machine Learning Techniques, in: Abu Dhabi International Petroleum Exhibition & Conference. *Society of Petroleum Engineers*. [10.2118/197651-MS](https://doi.org/10.2118/197651-MS)
- Sudakov, O., Burnaev, E., Koroteev, D., 2019. Driving digital rock towards machine learning: Predicting permeability with gradient boosting and deep neural networks. *Computers & Geosciences* 127, 91–98. [10.1016/J.CAGEO.2019.02.002](https://doi.org/10.1016/J.CAGEO.2019.02.002)
- Verri, I., Della Torre, A., Montenegro, G., Onorati, A., Duca, S., Mora, C.A., Radaelli, F., Trombin, G., 2017. Development of a Digital Rock Physics workflow for the analysis of sandstones and tight rocks. *Journal of Petroleum Science and Engineering* 156, 790–800. [10.1016/j.petro.2017.06.053](https://doi.org/10.1016/j.petro.2017.06.053)

- Wang, W., Fan, D., Sheng, G., Chen, Z., Su, Y., 2019. A review of analytical and semi-analytical fluid flow models for ultra-tight hydrocarbon reservoirs. *Fuel* 256, **115737**. [10.1016/j.fuel.2019.115737](https://doi.org/10.1016/j.fuel.2019.115737)
- Yakimchuk, I., Evseev, N., Korobkov, D., Varfolomeev, I., Dinariev, O., Khan, V., Koroteev, D., Orlov, D., Muravleva, E., Belozarov, B., Krutko, V., Kondratev, A., 2019. Permeability and Porosity Study of Achimov Formation Using Digital Core Analysis, in: SPE Russian Petroleum Technology Conference. *Society of Petroleum Engineers*. [10.2118/196928-MS](https://doi.org/10.2118/196928-MS)
- Yu, W., Sepehrnoori, K., Patzek, T.W., 2016. Modeling Gas Adsorption in Marcellus Shale With Langmuir and BET Isotherms. *SPE Journal* 21, 589–600. [10.2118/170801-PA](https://doi.org/10.2118/170801-PA)
- Zaitoun, N.M., Awl, M.J., 2015. Survey on Image Segmentation Techniques. *Procedia Computer Science* 65, 797–800. [10.1016/j.procs.2015.09.027](https://doi.org/10.1016/j.procs.2015.09.027)
- Zhang, Y., Mostaghimi, P., Armstrong, R.T., 2019. Multiscale characterization of shale diffusivity using time-lapsed X-ray computed tomography and pore-level simulations. *Journal of Petroleum Science and Engineering* 182, **106271**. [10.1016/j.petrol.2019.106271](https://doi.org/10.1016/j.petrol.2019.106271)